Characterization of Cerium(IV) Oxide Ultrafine Particles Prepared Using Reversed Micelles

Toshiyuki Masui, Kazuyasu Fujiwara, Ken-ichi Machida, and Gin-ya Adachi*

Department of Applied Chemistry, Faculty of Engineering, Osaka University, Yamadaoka 2-1, Suita, Osaka 565, Japan

Takao Sakata and Hirotaro Mori

Research Center for Ultra-High Voltage Electron Microscopy, Osaka University, Yamadaoka 2-1, Suita, Osaka 565, Japan

Received May 12, 1997. Revised Manuscript Received August 12, 1997[⊗]

Cerium(IV) oxide ultrafine particles were prepared using a reaction within reversed micelles, which was known as a microemulsion method. The ultrafine particles, which were obtained by mixing the water-in-oil microemulsions containing cerium nitrate solution with those of ammonium hydroxide, were characterized by high-resolution electron microscope (HREM) observations. HREM micrographs revealed that nanometer-sized CeO_2 particles were formed, and their shapes were uniform. Selected-area electron diffraction patterns of the particles were completely indexed as those of cerium(IV) oxide with the cubic fluorite structure, and the lattice constant calculated from radii of Debye−Sherrer rings was 0.541 nm. Most of the particles were distributed between 2 and 6 nm, and the mean particle size obtained in this method was between 2.6 and 4.1 nm. The size of 2.6 nm is the smallest among the values ever reported for CeO_2 particles. Both direct and indirect optical energy gaps of the particles were independent of the mean particle size, and their values were almost the same as that of the bulk material, suggesting that there was no quantum size effect of the CeO_2 ultrafine particles. However, the alumina-supported ultrafine CeO_2 catalysts prepared by a microemulsion method showed much higher CO oxidation activities than those prepared by a coprecipitation method.

1. Introduction

Cerium oxide is a major compound in the useful rare earth family and has been applied as one of practically used glass-polishing materials, ultraviolet absorbent, and automotive exhaust promoter. In recent years, ultrafine nanometer-sized particles have attracted much attention due to the physical and chemical properties which are significantly different from those of bulk materials.[1] Fine particles of cerium oxide with very small size have great potential to become new materials that are useful for fine UV absorbent and high-activity catalysts. Many workers have prepared them using various methods such as inert gas condensation of Ce metal (matrix isolation) followed by oxidation by O_2 gas,[2] hydrolysis of cerium isopropoxide (alkoxide process),[3] process of homogeneous precipitation using urea or hexamethylenetetramine,[4] forced hydrolysis of cerium salts in the presence of diluted sulfuric acid,[5] hydrothermal synthesis technique,[6−8] and electrochemical synthesis.[9] In these references, some of the properties such as sinterability of the particles, thermal stability of specific surface area, and catalytic properties have also been investigated.

The method described here is based on the use of microemulsions as reactors to obtain ultrafine and monodispersed nanoparticles. The microemulsion is generally defined as a thermodynamically stable system composed of two immiscible liquids and a surfactant. In water-in-oil microemulsions, the aqueous phase is dispersed as nanosize water droplets covered with a monolayer film of surfactant and cosurfactant molecules in a continuous nonpolar organic solvent such as hydrocarbon. Not only water but also aqueous solutions of metal salts or ammonia water can be soluble within the reversed micelles. These aqueous droplets encapsulated with surfactant molecules can continuously exchange their contents with one another when they collide.[10,11] Therefore, if two water-in-oil microemulsions (one dissolves reactants A and another dissolves

* To whom correspondence should be addressed.

[⊗] Abstract published in *Advance ACS Abstracts,* September 15, 1997.

(1) Andres, R. P.; Averback, R. S.; Brown, W. L.; Brus, L. E.; Goddard, W. A., III; Kaldor, A.; Louie, S. G.; Moscovits, M.; Peercy, P. S.; Riley, S. J.; Siegel, R. W.; Spaepen, F.; Wang, Y. *J. Mater. Res.* **1989**, *4*, 704.
(2) Tschöpe, A.; Ying, J. Y. *Nanostruct. Mater.* **1994**, *4*, 617.
(3) Imoto, F.; Nanataki, T.; Kaneko, S. *Ceram. Trans.* **1988**, *1*, 204.
(4) Chen, P. L.; Chen, I. W. *J. Am. Ceram. Soc.* **1993**, *76*, 1577.
(5) Hsu, W. P.; Rönnqist, L; Matijevic, E. *Langmuir* **1988**, *4*, 31.
(6) Zhou, Y. C.; Rahaman, M. N. *J. Mater. Res.* **1993**, *8*, 1680.
(7) Hirano, M.; Kato, E. *J. Am. Ceram. Soc.* **1996**, *79*, 777.
(8) Chebgyun, W.; Yitai, Q.; Changsui, W.; Li, Y.; Guiwen, Z. *Mater. Sci. Eng.* **1996**, *B39*, 160.
(9) Zhou, Y.; Phillips, R. J.; Switzer, J. A. *J. Am. Ceram. Soc.* **1995**, *78*, 981.
(10) Eicke, H. F.; Shepherd, J. C. W.; Sternemann, A. *J. Colloid Interface Sci.* **1976**, *56*, 168.
(11) Fletcher, P. D. I.; Howe, A. M.; Robinson, B. H. *J. Chem. Phys., Faraday Trans. 1* **1987**, *87*, 877.
(12) Boutonnet, M.; Kizling, J.; Stenius, P.; Maire, G. *Colloids Surf.* **1982**, *5*, 209.
(13) Petit, C. *J. Phys. Chem.* **1993**, *97*, 6961.
(14) Petit, C.; Lixon, P.; Pileni, M. P. *J. Phys. Chem.* **1993**, *97*, 12974.
(15) Pileni, M. P.; Lisiecki, I. *Colloids Surf.* **1993**, *80*, 63.
(16) Gobe, M.; Kon-no, K.; Kandori, K.; Kitahara, A. *J. Colloid Interface Sci.* **1983**, *93*, 293.

S0897-4756(97)00359-1 CCC: $14.00

reactants B) are mixed, a reaction between them takes place during collisions of the water droplets in the microemulsions.

According to the above method, several studies have been carried out in recent years, and monodisperse ultrafine particles of metals[12−15] and oxides[16,17] were synthesized in the dispersed phase of water-in-oil (W/O) microemulsion. Using this method enables us to obtain the particles with uniform small size and narrow size distribution, because the reaction field is limited inside of the fine reversed micelles. Nevertheless, rare earth compounds have not been synthesized by this method.

In the present study, we employed the microemulsion method to prepare the nanometer-sized cerium oxide ultrafine particles, and their size, morphology, and distribution were characterized with a high-resolution transmission electron microscopy (HREM). Also, the effect of fine size was estimated with the observation of the ultraviolet−visible absorption property and catalytic behavior for CO oxidation of the particles.

2. Experimental Section

2.1. Chemicals. The materials used in this work were of the best quality commercially available. Polyoxyethylene(10) octylphenyl ether (OP-10, Wako Pure Chemical Industries Ltd.), cyclohexane (Kanto Chemical Co., Inc.), *n*-hexyl alcohol (Wako Pure Chemical Industries Ltd.), ammonia water (Nacalai Tesque, Inc.), acetone (Kanto Chemical Co., Inc.), and methyl alcohol (Wako Pure Chemical Industries Ltd.) were used without further purification. Also, the aqueous solution of cerium nitrate (Shin-Nippon Kinzoku Kagaku Co., Ltd.), aqueous solution of zirconyl nitrate (Shin-Nippon Kinzoku Kagaku Co., Ltd.), and γ-aluminum oxide (Shin-Nippon Kinzoku Kagaku Co., Ltd., Brunauer−Emmett−Teller (BET) Specific surface area: 150 $m^2\ g^{-1}$) used were of high purity over 99.9%.

2.2. Synthesis. The preparation of the ultrafine cerium oxide particles was achieved by mixing two microemulsions containing cerium nitrate and ammonium hydroxide. The microemulsion system used in this work was composed of OP-10, cyclohexane, *n*-hexyl alcohol, and water solution. As OP-10 was only slightly soluble in cyclohexane solely, *n*-hexyl alcohol was added as a cosurfactant.

A microemulsion containing cerium salt was prepared as follows. First, OP-10 was mixed with *n*-hexyl alcohol in the molar ratio 1:6.3 (weight ratio 1:1), and 12−180 mL of this solution was added to 200 mL of cyclohexane with stirring until the mixture became transparent. Then, 2 mL of a cerium nitrate aqueous solution was added into the mixture and stirred until it became transparent again. The content of cerium ion was varied so as to correspond to 0.093, 0.23, 0.46, and 0.93 mol L^{-1}. Another microemulsion solubilizing 15 mol L^{-1} ammonium hydroxide was also prepared under the same procedure conditions described above. Then, the microemulsion containing cerium nitrate solution was mixed with another microemulsion containing ammonium hydroxide. The reaction mixture was stirred until a colloidal suspension formed. The particles were separated by centrifuging at a rate between 2.0×10^4 and 2.5×10^4 rpm for 1 h. After being successively washed with methyl alcohol, deionized water, and acetone by ultrasonic agitation, the fine powders were dried by freeze-drying and vacuum-drying.

The CeO_2/Al_2O_3 catalyst was prepared by almost the same procedure as that used for preparing the particles only. Twelve milliliters of the OP-10 and *n*-hexyl alcohol mixture, 40 mL of cyclohexane, and 2 mL of a 0.93 mol L^{-1} cerium nitrate aqueous solution were mixed with stirring until the mixture became transparent. Another microemulsion solubilizing 15 mol L^{-1} ammonium hydroxide was also prepared with dispersed γ-aluminum oxide powders. Then, the microemulsion that contained the cerium nitrate solution was added into the solution containing ammonium hydroxide and γ-Al_2O_3 powders. In this process, the prepared CeO_2 ultrafine particles were supported on the surface of γ-Al_2O_3. The loading of the CeO_2 was 16.7 mol % (molar ratio of $CeO_2/Al_2O_3 = 1/6$). After the reaction mixture was stirred for 3 h, the suspension was centrifuged at $5 \times 10^3 - 1 \times 10^4$ rpm for 1 h, and catalyst powder was obtained. The catalyst was washed successively with methyl alcohol, deionized water, and acetone. Finally, the powder was dried by the freeze-drying method followed by vacuum-drying at 423 K for 1 h. The catalyst prepared in this method is denoted by ME catalyst hereafter. In addition, we prepared a coprecipitated catalyst to compare CO oxidation activities with that of a catalyst prepared by a microemulsion method. The coprecipitated catalyst was prepared by mixing of a cerium nitrate solution with ammonium hydroxide in which γ-aluminum oxide powders were dispersed and was washed and dried in a similar way to the ME catalyst. The catalyst prepared in a coprecipitated method is denoted by CP catalyst hereafter.

2.3. Instruments and Characterization. The ultrafine powders prepared by the microemulsion method were characterized by X-ray diffraction (XRD) using Cu*K*α radiation (MAC Science M18XHF-SHA), high-resolution transmission electron microscopy (Hitachi H-9000), and differential thermal analysis (Rigaku TAS-100). The particle size and distribution were determined by measuring the maximum diameter of more than 200 particles on the HREM micrographs. Specific surface areas of the catalysts were measured by a conventional (BET) nitrogen adsorption method (Micromeritics Flow Sorb II 2300).

UV−vis absorption spectra of the cerium oxide particles dispersed in methyl alcohol were recorded using a Shimadzu UV-2000 spectrometer using a quartz cuvette (1 cm path length). Methyl alcohol was used as reference. The catalytic reactions for CO oxidation were carried out with 0.50 g of the catalyst in a conventional fixed-bed quartz tube reactor (10 mm o.d.) at 323−973 K. The inlet gas composition was 2% CO and 16% O_2 with He as balance, and the flow rate was adjusted to 25 mL min^{-1}. Products were analyzed by gas chromatography (Shimadzu GC-8A), and the CO oxidation activity of the ME catalyst was compared with that of the CP catalyst, both before and after the calcination at 1273 K in air for 5 h.

3. Results and Discussion

3.1. Characteristics of the CeO_2 Ultrafine Particles. The yield for the microemulsion process was between 60 and 70%, and it was confirmed from differential thermal analysis data that surfactant did not remain in the samples. During the process, we observed systematic changes in color of the precipitated particles in some cases. After the cerium nitrate microemulsion was mixed with the ammonium hydroxide microemulsion, the colorless transparent original solution immediately became translucent and gradually precipitated orange-colored fine particles. A colorless and clear supernatant was formed after the precipitation, but the further color variance of the precipitate was observed. First, the color of the fine particles changed from orange to purple in about 30 min. Subsequently, the color of the precipitate gradually turned into pale purple, but the color variance was slower than the first change. Moreover, the color slowly changed to light yellow, and it took about 3 h to change completely. The wet centrifuged precipitate also appeared light yellow, but finally the freeze-dried powders were light brown.

These changes in color were observed in the cases that the particles were synthesized in low surfactant con-

(17) Ramamurthi, S. D.; Xu, Z.; Payne, D. A. *J. Am. Ceram. Soc.* **1990**, *73*, 2760.

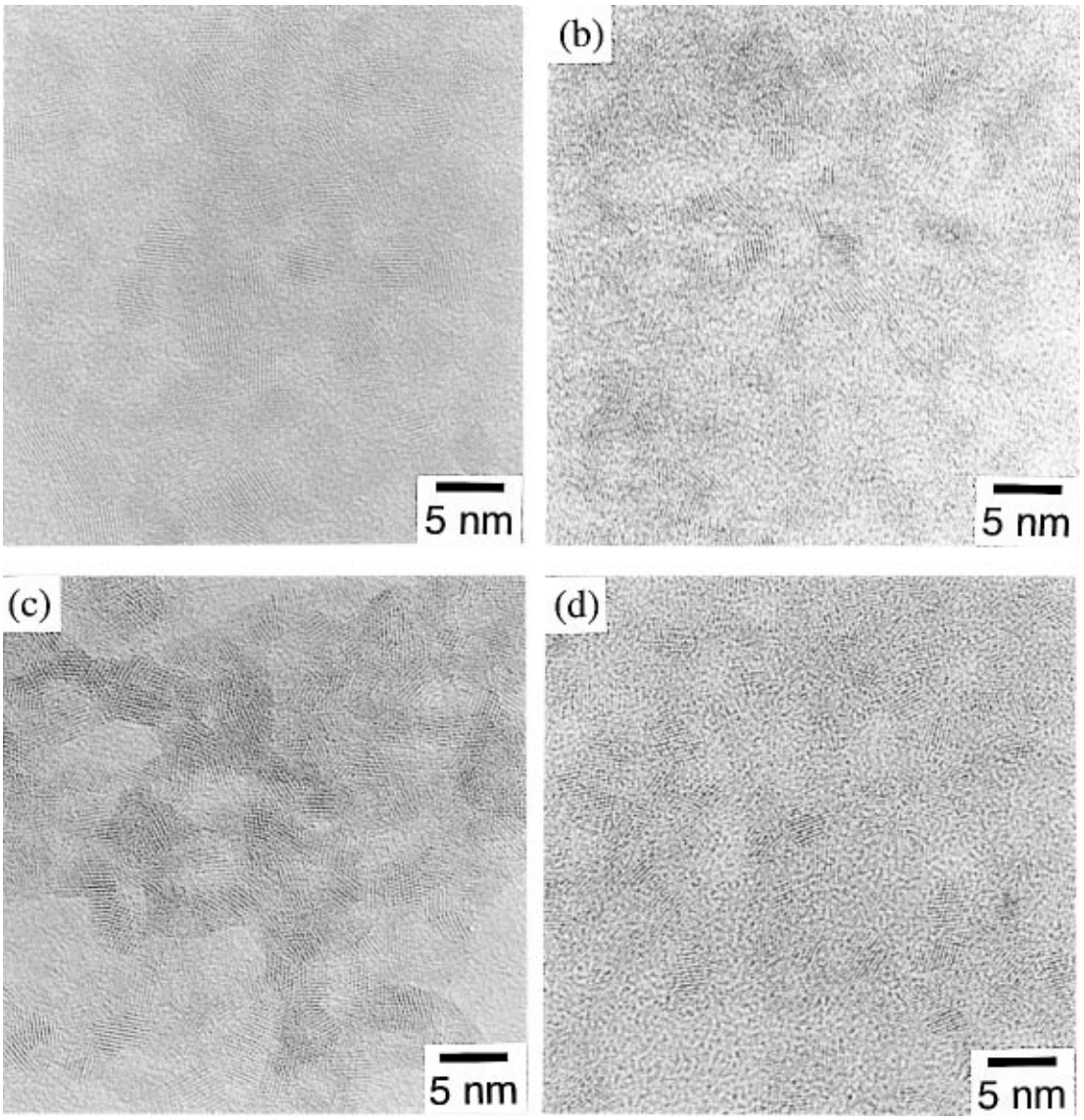

Figure 1. High-resolution electron micrograph of CeO_2 ultrafine particles by microemulsion method: These particles were prepared from 0.93 mol L^{-1} cerium nitrate solution at (a) Rw = 15, (b) Rw = 1.5, or from 0.093 mol L^{-1} cerium nitrate solution at (c) Rw = 15, (d) Rw = 1.5.

centration. On the contrary, there was no color variance of the precipitate in high surfactant concentration. That is, the originally colorless transparent solution immediately only became orange-colored translucent and precipitation did not occur. This is due to the fact that the particles prepared within reversed micelles are stable in the solution at high surfactant concentration.[18] The color of the wet centrifuged particles also appeared orange, but the final freeze-dried powders were light brown.

Figure 1 shows high-resolution electron micrographs of the ultrafine cerium(IV) oxide particles prepared by the microemulsion method. The content of water pool in reversed micelles is defined as the ratio of water to surfactant concentration, that is, Rw = $[H_2O]/[OP\text{-}10]$. In any case, it was evident from this figure that the particle size was very small, and the particle size decreased upon decreasing from Rw = 15 to Rw = 1.5, although the particles somewhat agglomerated one another. HREM also showed well-defined crystallites and their lattice images for most particles. BET specific surface area of the powders were between 153 and 185 $m^2\ g^{-1}$. Assuming that all particles were spheres, their sizes calculated from the BET specific surface area were between 4.4 and 5.4 nm. These values seemed to be slightly larger than the HREM data because the dried powders were composed of agglomerated ultrafine powders.

X-ray powder diffraction of the CeO_2 nanoparticles obtained in this study have patterns consistent with the cubic phases. However, the width of the peaks were broad because of their small particle size. Therefore, in this case electron diffraction is a more valuable technique for characterization, and information on the lattice parameter and crystal structure of the particles was obtained from the selected-area electron diffraction patterns. Figure 2 shows the diffraction patterns and the Debye−Sherrer rings of the particles. They can be consistently indexed as those of cerium(IV) oxide with the cubic fluorite structure, and the lattice constant

(18) Sano, T.; Kawai, T.; Kon-no, K. *Proceedings of the International Conference on Color Materials;* Osaka, Japan, 1992, p 120.

(19) X-ray Powder Diffraction Standards, ASTM, Philadelphia, PA. Card 34-394 (CeO_2).

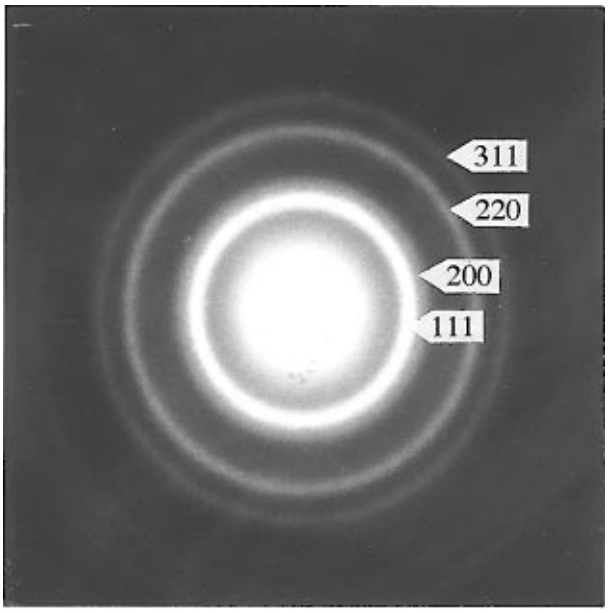

Figure 2. Electron diffraction pattern of CeO_2 ultrafine particles prepared by the microemulsion method.

calculated from the radii of rings was 0.541 nm. This value was in good agreement with that given in the literature.[19]

These results presented in Figures 1 and 2 showed that the precipitate from the reaction between cerium nitrate and ammonium hydroxide solutions in reversed micelles already exhibited the patterns of the CeO_2 crystallite. Chen et al.[4] previously reported that same behavior was observed by the direct reaction of cerium nitrate and ammonium hydroxide in the homogeneous precipitation method. In the literature, they concluded that this might be due to the addition of a large amount of NH_4OH because very high pH value was favorable for the oxidation of Ce^{3+} to Ce^{4+}. The results in this study would be due to the same reason except there is a different point from their result. The difference is the color change of the particles. In our results, the particle's color completely changed to light yellow before drying, while the homogeneous precipitated particles changed only after drying. The CeO_2 particles prepared by our method were much smaller than the precipitated ones and were composed of 250−900 cerium ions, that is, 40−60% of them were present at the surface. In our sample, therefore, the surface energy was much higher and the oxidation of Ce^{3+} to Ce^{4+} had to be more completely driven than was the precipitated one.

3.2. Size Distribution and Mean Size of CeO_2 Particles. In the microemulsion method, the final size of the cerium oxide particles is restricted because the chemical reaction of cerium salt solution with ammonia water takes place inside the water droplets within the reversed micelles. Once the particles became a critical size in the water droplets, the surfactant molecules adsorbed on the surface of the particles to protect them against the further particle growth.

Figure 3 shows size distribution histograms of the cerium oxide particles prepared by using reversed micelles with different Rw values. At high water content, Rw = 15, the size distribution and mean particle size of the cerium oxide particles were relatively large. In contrast, at low water content, Rw = 0.5, the size distribution was very narrow and mean size was very small. The particle size change with the Rw value is shown in Figure 4, and the data are summarized in Table 1. As shown in these figures and the table, the mean particle size was decreased from 4.1 to 2.9 nm when we used 0.93 mol L^{-1} $Ce(NO_3)_3$ as starting material. In the case of 0.093 mol L^{-1} $Ce(NO_3)_3$, the mean particle size was decreased from 3.4 to 2.6 nm. Here the mean size, 2.6 nm, was the smallest among the previous values reported for CeO_2 particles prepared by other methods.

The water droplet within reversed micelles is classified into two types of water.[20] One is the water which strongly interacts with the surfactant or cosurfactant molecules, and another is the water which behaves as bulk water. At low Rw, most of water is the former, and at high Rw, both the former and the latter are present. In addition, it is known that the size of both reversed micelles and water droplets increase with Rw value. As a result, the final size of the nanometer-scale particles can be varied by changing the amount of water solution solubilized in the system.

In the case of Cu nanoparticles preparation using Aerosol OT as a surfactant, the change in the particle size with water content was elucidated by Pileni and co-workers.[14,15,21] They have explained the reason in terms of the facial water structure: At low water content, metal ions within reversed micelles strongly associate with surfactant or cosurfactant molecules, and they are not totally reacted. Our results support this explanation because the mean particle size did not decrease below 2.6 nm for the samples prepared from 0.093 mol L^{-1} cerium nitrate solution (Figure 4b). This suggests that the size of 2.6 nm is the lower limit in the present system. On the other hand, the increase in the water content induces the extra free metal ions which react with reactant. This is responsible for the increase of the mean particle size. Electrostatic interaction between the surfactant and metal ions influence the reaction rate, but the balance in these remains constant upon increasing the water content. In addition, it is possible that more than one particle is formed in a reversed micelle at high Rw because the reaction space increases with water content.[21] Therefore, at high water content above Rw = 9, the particle size was almost constant.

As mentioned above, it is known that the sizes of both the reversed micelle and the water droplet depend on the Rw value. Therefore, if the concentration ratio of water to surfactant in W/O microemulsions is constant, the size of the particles seems to depend on the concentration of cerium ion. The distribution histograms of the cerium oxide ultrafine particles prepared at Rw = 15 are shown in Figure 5. The concentration of cerium nitrate solution was changed so as to correspond to 0.093, 0.23, 0.46, and 0.93 mol L^{-1}. In all cases, most of the particles distributed in a range of 1.5−6.0 nm, and the particle distribution range was almost independent of the cerium nitrate concentration. However, as the concentration of cerium nitrate increased, the peak of the distribution was slightly shifted to the larger particle size side. The particle sizes of the cerium oxide samples prepared from the solutions with various concentrations of Ce^{3+} ion are summarized with stan-

(20) Zinsli, P. F. *J. Phys. Chem.* **1979**, *83*, 3223.
(21) Pileni, M. P. *J. Phys. Chem.* **1993**, *97*, 6961.

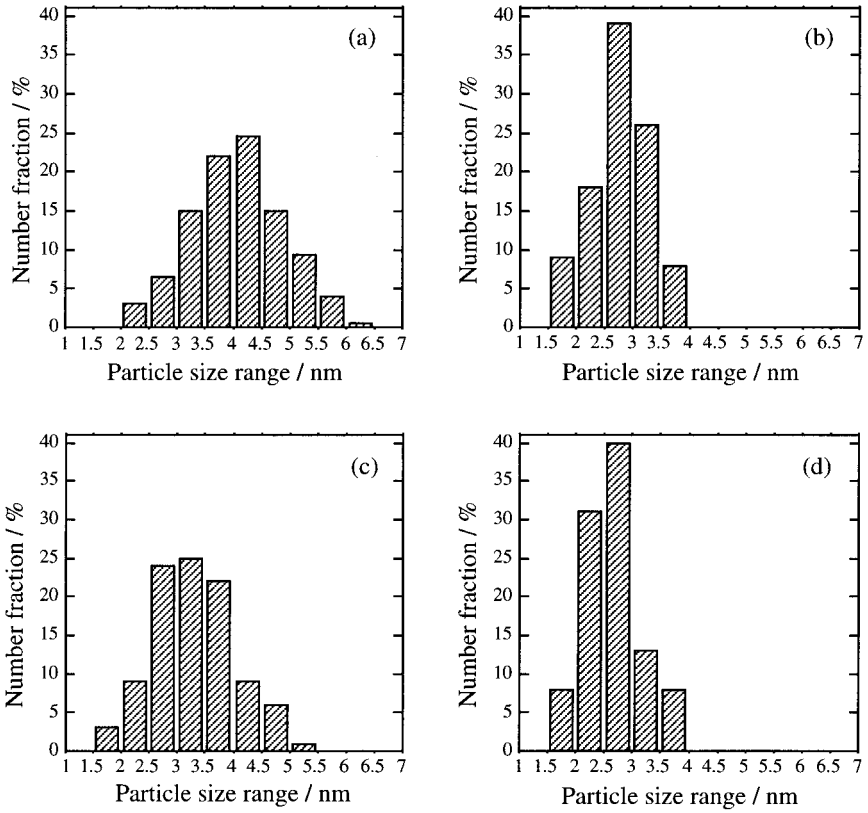

Figure 3. Particle size distribution histograms of CeO_2 ultrafine particles prepared from 0.93 mol L^{-1} cerium nitrate solution at (a) Rw = 15, (b) Rw = 0.5, or from 0.093 mol L^{-1} cerium nitrate solution at (c) Rw = 15, (d) Rw = 0.5.

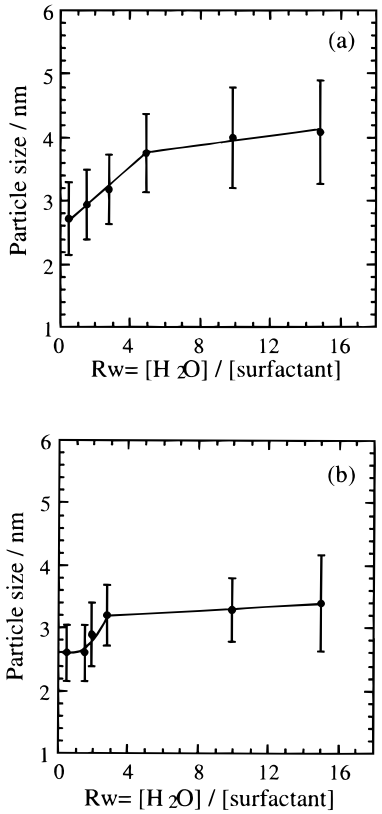

Figure 4. Mean particle size change of CeO_2 ultrafine particles prepared from (a) 0.93 mol L^{-1} and (b) 0.093 mol L^{-1} cerium nitrate solution at various Rw values.

dard deviations in Table 2. It is found that the higher the concentration of the cerium nitrate solution, the larger the mean CeO_2 particle size prepared. However, the largest mean size was not above 5 nm.

Table 1. Mean Particle Size of Cerium(IV) Oxide for Different Rw Values

	prepared from 0.93 mol L^{-1} $Ce(NO_3)_3$		prepared from 0.093 mol L^{-1} $Ce(NO_3)_3$	
Rw	mean particle size (nm)	standard deviation (nm)	mean particle size (nm)	standard deviation (nm)
0.5	2.7	0.57	2.6	0.46
1.5	2.9	0.55	2.6	0.45
1.9			2.9	0.50
2.8	3.2	0.56	3.2	0.49
4.9	3.8	0.62		
9.9	4.0	0.80	3.3	0.51
15	4.1	0.82	3.4	0.77

3.3. Absorption Spectra and Optical Bandgap of Ultrafine CeO_2 Particles. The ultrafine CeO_2 particles prepared in this study are materials that can prevent some damage from ultraviolet rays because they show strong absorption below 400 nm caused by charge-transfer bands and block damage by UV radiation. Therefore, it is very important to characterize the optical properties of CeO_2 ultrafine particles for identification whether there is a specificity based on ultrafine size or not; however, there was no report on them.

Absorption spectra of the CeO_2 ultrafine particles dispersed in methyl alcohol, which were measured by taking into account the methyl alcohol for blank, are shown in Figure 6. The spectrum for the specimen with the mean size of 2.6 nm is represented by a solid line and that of 4.1 nm was corresponds to a dashed line. The concentration of the CeO_2 ultrafine particles was 4.6×10^{-4} mol L^{-1} for both solutions, and these suspensions were transparent and colored with light

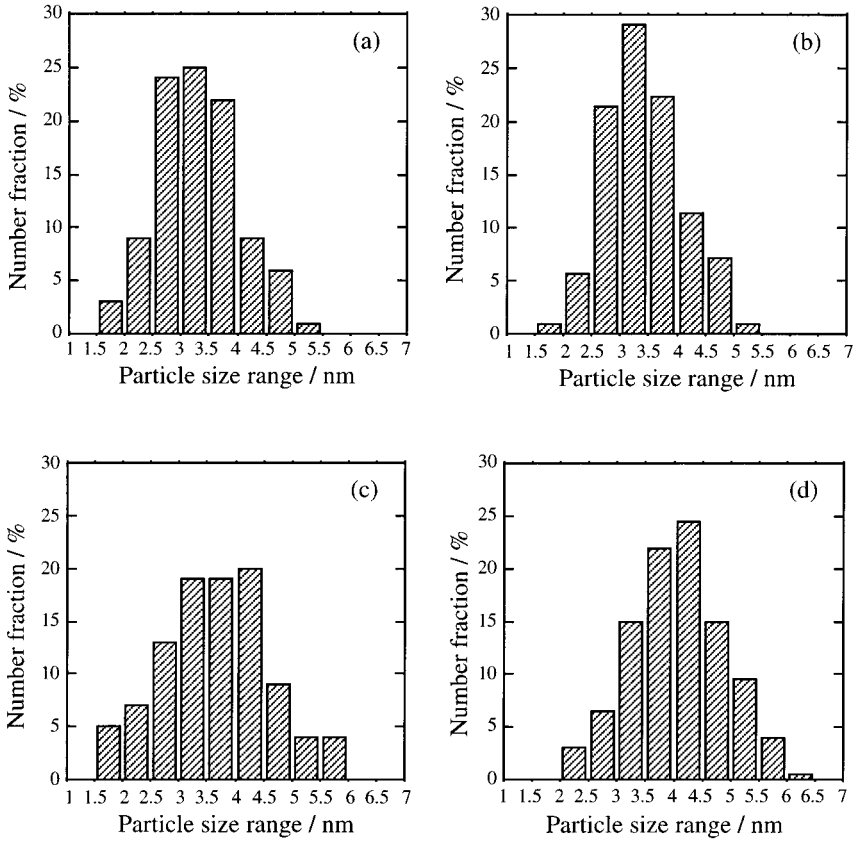

Figure 5. Particle size distribution of CeO_2 ultrafine particles at Rw = 15 prepared from (a) 0.093, (b) 0.23, (c) 0.46, and (d) 0.93 mol L^{-1} cerium nitrate solution.

Table 2. Mean Particle Size of Cerium(IV) Oxide Prepared at Rw = 15 for Different Concentrations of Reactants

$[Ce(NO_3)_3]$ (mol L^{-1})	mean particle size (nm)	standard deviation (nm)
0.093	3.4	0.77
0.23	3.5	0.76
0.46	3.7	0.96
0.93	4.1	0.82

yellow. Although the mean size of the particles decreased, the absorption edge obtained from the intersection of the tangent with the wavelength axis showed a weak blue shift.

The bandgap energy E_g for the CeO_2 particles is determined by extrapolation to the zero absorption coefficient which is calculated from the following equation[22]

$$\alpha = (2.303 \times 10^3 A\rho)/lC \quad (1)$$

where A is the absorbance of a sample, $\log(I_0/I_t)$; ρ is the density of CeO_2, 7.28 g cm^{-3}; C is the loading of the particles in g L^{-1}; and l is the path length. The optical absorption coefficient α near the absorption edge for indirect interband transitions is shown in the following equation[23]

$$\alpha \propto \frac{(h\nu + E_p - E_i)^2}{e^{(h\nu/kT)} - 1} + \frac{(h\nu - E_p - E_i)^2 e^{(h\nu/kT)}}{e^{(h\nu/kT)} - 1} \quad (2)$$

where E_i is the bandgap energy for indirect transitions, $h\nu$ is the photon energy, and E_p is the phonon energy. For direct transitions, the optical absorption coefficient

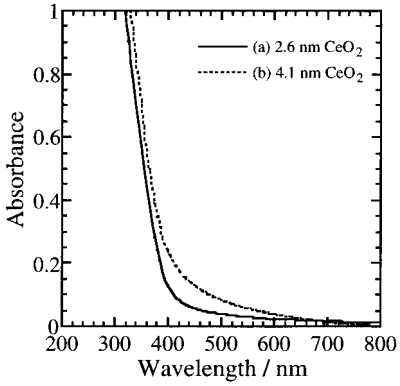

Figure 6. Absorbance spectra of CeO_2 ultrafine particles dispersed in methyl alcohol: The mean particle sizes are (a) 2.6 nm and (b) 4.1 nm, respectively.

near the absorption edge is shown in the following equation[23]

$$\alpha \propto (h\nu - E_d)^{1/2}/h\nu \quad (3)$$

where E_d is the bandgap energy for direct transitions.

Figure 7 shows the plots of $\alpha^{1/2}$ vs the photon energy for the CeO_2 particles with mean sizes of 2.6 and 4.1 nm. A linear extrapolation toward zero absorption gives E_i corresponding to indirect allowed transitions. The E_i values were 2.87 eV for the sample with 2.6 nm and 2.73 eV for that with 4.1 nm, respectively.

The plots of $(\alpha h\nu)^2$ vs the photon energy for the CeO_2 particles with the mean sizes of 2.6 and 4.1 nm are

(22) Serpone, N.; Lawless, D.; Khairutdinov, R. *J. Phys. Chem.* **1995**, *99*, 16646.

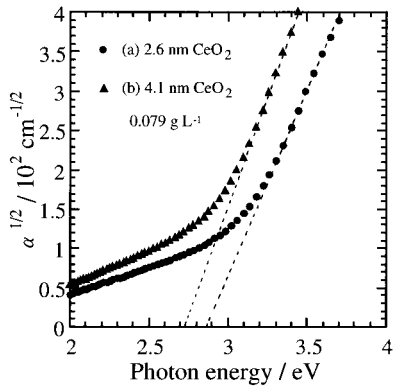

Figure 7. Plots of $\alpha^{1/2}$ vs photon energy for the CeO_2 particles dispersed in methyl alcohol: the mean particle sizes are (a) 2.6 nm and (b) 4.1 nm, respectively.

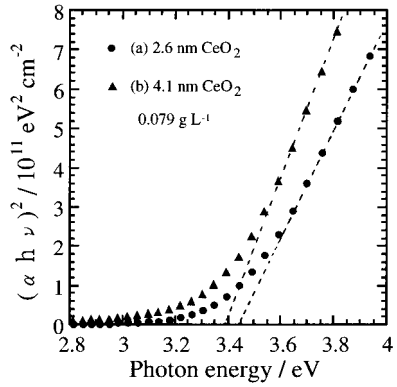

Figure 8. Plots of $(\alpha h\nu)^2$ vs photon energy for the CeO_2 particles dispersed in methyl alcohol: The mean particle sizes are (a) 2.6 nm and (b) 4.1 nm, respectively.

shown in Figure 8. Also, the intersection of the extrapolated linear portions gives the bandgap E_d for direct transitions, and the bandgap values of them were 3.44 and 3.38 eV, respectively. Both of the indirect and direct bandgap energies increased with the decrease in the mean particle size, but the difference between them was small.

There are some reports on the bandgap energy of CeO_2 thin film. Hogarth and Al-Dhhan[24] reported the E_i value to be 3.10 eV. Sundaram and Wahid[25] evaluated the bandgap energy for CeO_2 films prepared by evaporation of Ce followed by oxidation through heating in O_2 to be between 3.02 and 3.20 eV and between 3.34 and 3.38 eV, energy for indirect and direct transitions, respectively. Similar results between 3.0 and 3.12 eV for indirect transition and between 3.5 and 3.6 eV for direct transition were reported by Orel and Orel[26] for CeO_2 thin films prepared by a sol−gel method. These values are close to those of this study.

Moreover, the present values were almost equal to those of the ultrafine CeO_2 particles prepared by the RAD process,[27] which was a thermal relaxation technique to prepare various ultrafine particles. The mean particle sizes obtained by the RAD process were 4.1 and 5.8 nm, which were larger than those prepared in this study. Nevertheless, their direct bandgap values calculated from eq 2 were 3.42 and 3.37 eV, respectively, and they were in fair agreement with those of the samples prepared in the present study.

From these results, a little increase of bandgap energy with deceasing particle size was not due to the quantum size effect because the bandgap energies obtained here were comparable to those of CeO_2 thin films[26,28] and the CeO_2-containing composite films[27] which were composed of nanosize CeO_2 crystalline particles. Therefore, we can conclude that there is no quantum size effect on the ultrafine CeO_2 particles at least over 2.6 nm.

3.4. Catalytic Activities of Ultrafine CeO_2 Particles Supported on Al_2O_3. As well as the ultraviolet absorbing property, it is known that cerium oxide shows high oxidation ability and oxygen storage capacity (OSC),[29] and the appearance of these functions is attributed to following two reasons. One is a low redox potential between Ce^{3+} and Ce^{4+}, and the other is its structure.[30] The stable structure of cerium oxide at atmospheric pressure and room temperature is the cubic fluorite structure in which oxygen ions do not have a close-packed structure. Owing to this structure, cerium oxide can easily form many oxygen vacancies while maintaining the basic crystal structure. Although nanoparticles of cerium oxide have a great potentiality to be a high active catalyst because half of the cerium ions in the particles were present at their surface, there were a few reports on some catalytic properties based on their fine size.[2,31] Then we focused on the improvement in catalytic properties with the use of nanosize CeO_2 catalysts.

Powder XRD patterns for the as-prepared ME and CP CeO_2/Al_2O_3 catalysts showed diffraction peaks assigned to CeO_2 and γ-Al_2O_3. The width of these peaks were broad because of their small crystalline sizes, but there were no differences between them. Although the crystallinity of both samples was improved to provide sharp diffraction peaks after the heat treatment in air at 1273 K for 5 h, there also were no clear differences between the ME and CP CeO_2 catalysts.

The catalytic activity tests for the ME and CP CeO_2/Al_2O_3 catalysts have been carried out to study the effect of small particle size and their preparation process on the oxidation of CO. Carbon dioxide was the only product for all catalysts. The activities of the ME and CP catalysts were compared in terms of their light off temperature corresponding to 50% conversion both before and after the heat treatment. The results are shown in Figure 9, and the overall activity data and BET specific surface areas are summarized in Table 3. Before the heat treatment, CO oxidation activity of the ME catalyst was higher than that of the CP one. After the heat treatment in air at 1273 K for 5 h, the activities of the ME and CP catalysts were decreased. This might be due to the sintering of the fine particles impregnated on Al_2O_3, since the surface areas of them considerably decreased by the heat treatment (Table 3). However,

(23) Van Leeuwen, R. A.; Hung, C.-J.; Kammler, D. R.; Switzer, J. A. *J. Phys. Chem.* **1995**, *99*, 15247.
(24) Hogarth, C. A.; Al-Dhhan, Z. T. *Phys. Stat. Sol. B.* **1986**, *137*, K157.
(25) Sundaram, K. B.; Wahid, P. *Phys. Stat. Sol. B.* **1990**, *161*, K63.
(26) Orel, Z. C.; Orel, B. *Phys. Stat. Sol. B.* **1994**, *186*, K33.
(27) Masui, T.; Machida, K.; Sakata, T.; Mori, H.; Adachi, G. *J. Alloys Compd.* **1997**, *256*, 97.
(28) Orel, Z. C.; Orel, B. *Sol. Energy Mater. Sol. Cells.* **1996**, *40*, 205.
(29) Yao, H.; Yu-Yao, Y. F. *J. Catal.* **1984**, *86*, 254.
(30) Haneda, M.; Mizushima, T.; Kakuta, N.; Ueno, A.; Sato, Y.; Matsuura, S.; Kasahara, K.; Sato, M. *Bull. Chem. Soc. Jpn.* **1993**, *66*, 1279.
(31) Tschöpe, A.; Liu, W.; Flytzani-Stephanopoulos, M.; Ying, J. Y. *J. Catal.* **1995**, *157*, 42.

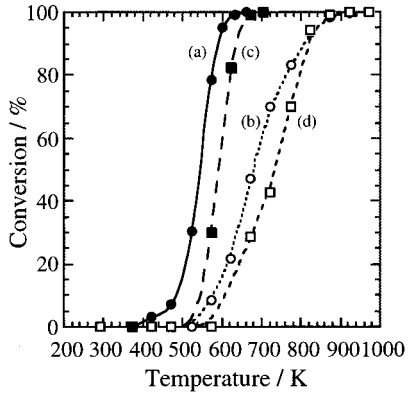

Figure 9. Catalytic activities for CO oxidation of (a) as-prepared ME CeO_2/Al_2O_3, (b) ME CeO_2/Al_2O_3 after being calcined at 1273 K for 5 h, (c) as-prepared CP CeO_2/Al_2O_3, and (d) CP CeO_2/Al_2O_3 after being calcined at 1273 K for 5 h. ME and CP represent that the catalysts were prepared by a microemulsion method and by a coprecipitation method, respectively.

Table 3. BET Surface Areas and Activity Data for the Investigated Catalysts[a]

sample	preheat temp, K	BET surface area/$m^2\ g^{-1}$	T, K (50%)[b]
CeO_2/Al_2O_3 prepared by microemulsion method	423	165	543
	1273	73	680
CeO_2/Al_2O_3 prepared by coprecipitation method	423	167	593
	1273	73	735

[a] Amount of catalyst = 0.5 g; reaction gas mixture He:CO:O_2 = 82:2:16; flow rate = 25 mL min^{-1}. [b] Temperature for 50% conversion of CO to CO_2.

the ME catalyst still showed a higher activity, and the reaction temperature over this catalyst was lower by about 55 K for 50% conversion than that over the CP catalysts. From these results, it is noted that the CeO_2/Al_2O_3 catalyst prepared by the microemulsion method shows higher activity despite the fact that its surface area is as low as that prepared by the coprecipitation method.

Haneda et al.[30] reported that the CeO_2/Al_2O_3 catalysts prepared by a sol−gel method using a needle boehmite sol derived from aluminum triisoproxide showed higher oxygen storage capacity after the H_2 reduction at 1173 K than those prepared by simple impregnation on an active alumina. They attributed the reason for high OSC to the high-dispersion state of CeO_2 particles and many oxygen vacancies, owing to the creation of new CeO_2 crystallite and CeO_{2-x} phases. Although the cause and the detailed mechanism of the high activities of ME catalyst have not been clear yet, they might be due to some effects such as fine size, morphology, and high OSC of the CeO_2 particles like the catalyst prepared by sol−gel method.

4. Conclusions

Nanometer-sized cerium(IV) oxide ultrafine particles were prepared by the microemulsion method and their size distribution was fairly narrow. We first made it clear that the size of the particles was controlled easily in the vital range under 5 nm only by changing the concentration of the starting materials. The smallest mean size of the cerium oxide, 2.6 nm, prepared in this study was smaller than any other values previously reported for CeO_2 particles.

The direct and indirect optical energy gaps of the particles obtained by the ultraviolet−visible spectrum measurement depended little on their mean size. Therefore, we conclude that there are no size quantization effects on the spectral properties of CeO_2 fine particles prepared in the present study.

The CeO_2/Al_2O_3 catalyst prepared by the microemulsion method showed a much higher CO oxidation activity than that prepared by the coprecipitation method, both before and after the heat treatment at 1273 K for 5 h. Because the surface area values of them were almost equal, the reason for the high catalytic activity might be due to some effects such as fine size, morphology, and high OSC of the CeO_2 particles.

Acknowledgment. The authors are indebted to Dr. Katsuji Tani, Mr. Akifumi Murase, and Professor Masao Nasu (Department of Pharmacy, Faculty of Pharmaceutical Sciences, Osaka University) for their assistance in centrifuging of the ultrafine particles. The authors also thank the Shin-Nippon Kinzoku Kagaku Co., Ltd. for their assistance in supplying the starting materials. This work was supported by Grant-in-Aid for Scientific Researches Numbers 06241106, 06241107, 08874090, and 06403021 from the Ministry of Education, Science, Sports, and Culture of Japan. T.M. is the recipient of a Research Fellowship of the Japan Society for the Promotion of Science for Young Scientists.

CM970359V